BIOCHEMICAL PHARMACOLOGY 74 (2007) 1587–1595

available at www.sciencedirect.com

ScienceDirect

journal homepage: www.elsevier.com/locate/biochempharm

The antiproliferative effects of phenoxodiol are associated with inhibition of plasma membrane electron transport in tumour cell lines and primary immune cells

P.M. Herst, T. Petersen, P. Jerram, J. Baty, M.V. Berridge *

Malaghan Institute of Medical Research, P.O. Box 7060, Wellington 6005, New Zealand

ARTICLE INFO

Article history:
Received 1 June 2007
Accepted 15 August 2007

Keywords:
Phenoxodiol
Anticancer drug
Mechanism of action
Plasma membrane electron transport
Apoptosis
T cells

ABSTRACT

Although the redox-active synthetic isoflavene, phenoxodiol, is in Phase 3 clinical trials for drug-resistant ovarian cancer, and in early stage clinical trials for prostate and cervical cancer, its primary molecular target is unknown. Nevertheless, phenoxodiol inhibits proliferation of many cancer cell lines and induces apoptosis by disrupting FLICE-inhibitory protein, FLIP, expression and by caspase-dependent and -independent degradation of the X-linked inhibitor of apoptosis, XIAP. In addition, phenoxodiol sensitizes drug-resistant tumour cells to anticancer drugs including paclitaxel, carboplatin and gemcitabine. Here, we investigate the effects of phenoxodiol on plasma membrane electron transport (PMET) and cell proliferation in human leukemic HL60 cells and mitochondrial gene knockout HL60ρ° cells that exhibit elevated PMET. Phenoxodiol inhibited PMET by both HL60 (IC_{50} 32 μM) and HL60ρ° (IC_{50} 70 μM) cells, and this was associated with inhibition of cell proliferation (IC_{50} of 2.8 and 6.7 μM, respectively), pan-caspase activation and apoptosis. Unexpectedly, phenoxodiol also inhibited PMET by activated murine splenic T cells (IC_{50} of 29 μM) as well as T cell proliferation (IC_{50} of 2.5 μM). In contrast, proliferation of WI-38 cells and HUVECs was only weakly affected by phenoxodiol. These results indicate that PMET may be a primary target for phenoxodiol in tumour cells and in activated T cells.

1. Introduction

The synthetic isoflavene, phenoxodiol [1], is in advanced clinical trials for the treatment of drug-resistant ovarian cancer and is in early stage trials for prostate and cervical cancer, both as a single agent and in chemo-sensitization settings. However, despite progression into clinical trials, the primary cellular target or targets of phenoxodiol remain elusive. Rather, the drug is often referred to as a multiple signal transduction regulator [2], a term consistent with its redox activity and multiple targets of the parent compound, genistein. Mechanistic studies have shown that phenoxodiol inhibits DNA topoisomerase II [1], and induces apoptosis in ovarian carcinoma [3,4] and melanoma cells [5]. Both caspase-dependent and -independent apoptosis have been described. With chemoresistant ovarian cancer cells, phenoxodiol induced early ubiquitination and degradation of the X-linked inhibitor of apoptosis, XIAP, via the proteosome [3,4], and disrupted expression of the FLICE-inhibitory protein, FLIP, through the Akt signal transduction pathway [4]. With other human cancer cell lines including head and neck and colon carcinoma, phenoxodiol induced caspase-independent apoptosis following G1 cell cycle arrest and this was associated with $p21^{WAF1}$ expression [6]. Induction of apoptosis by anticancer drugs is often a consequence of a primary site or sites of action physically distinct from the pro-apoptotic machinery

* *Corresponding author*. Tel.: +64 4 499 6914x825; fax: +64 4 499 6915.
E-mail address: mberridge@malaghan.org.nz (M.V. Berridge).
0006-2952/$ – see front matter
doi:10.1016/j.bcp.2007.08.019

rather than being a direct target. Therefore, understanding the primary molecular target and the linkage of this target to key components of apoptotic pathways is central to optimizing drug development and usage.

Fine control of the intracellular redox status of cells is critical for cell viability, growth and function. Perturbation of key redox couples such as the NADH/NAD^+ ratio, glutathione balance and membrane ubiquinone redox status and content can have profound effects on cells resulting in apoptosis [7,8]. Small redox-active amphipathic molecules such as phenoxodiol may disrupt essential redox cycling at many different levels within cells and their membranes. Because phenoxodiol is poorly water-soluble and requires the use of organic solvents, it will have a tendency to partition in membrane systems. This suggests that redox-active molecules in membranes may be primary targets for phenoxodiol action. Two main membrane systems orchestrate the bioenergetic status of cells. The inner mitochondrial membrane contains an electron transport system that is responsible for generating the membrane potential that drives most ATP production via oxidative phosphorylation. Ubiquinone is an essential redox-active mediator of mitochondrial electron transport (MET), shuttling electrons from Complexes I and II to Complex III. In the absence of mitochondrial electron transport, cells must rely on glycolysis to generate ATP. Increasing evidence indicates that the plasma membrane also contains an essential electron transport system that utilizes ubiquinone as a one electron acceptor and donor [9,10], and that this system may support glycolytic ATP production by oxidizing cytosolic NADH [11,12], a role usually attributed to lactate dehydrogenase (LDH). This suggests that plasma membrane electron transport (PMET) may be a primary site of action for the anticancer activity of redox-active lipophilic flavonoids such as phenoxodiol, catechins like epigallocatechin gallate, resveratrol and quinone-containing anticancer drugs such as doxorubicin.

Phenoxodiol was recently shown to bind with high affinity to a purified recombinant NADH-oxidase, compromising its ability to oxidize both NADH and ubiquinol and to catalyze protein disulfide–thiol interchange activity [13]. This protein is a truncated form of a tumour-specific cell surface NADH-oxidase, tNOX, thought to be involved in the transfer of electrons from intracellular NADH to an extracellular acceptor via plasma membrane ubiquinone [14,15]. These effects of phenoxodiol were shown to be associated with inhibition of HeLa cell enlargement and growth [13]. In contrast, activity of the constitutively-expressed cell surface NADH-oxidase, CNOX, present on both cancer and non-cancer cells was said to be unaffected by phenoxodiol.

In order to directly assess the effects of phenoxodiol on PMET, we have used mitochondrial gene knockout (ρ°) cells [11,16] in which bioactivity can be attributed to interaction with redox-sensitive systems other than MET, greatly simplifying interpretation of results. Using this system, we investigated the effects of phenoxodiol on PMET and cell proliferation in human leukemic HL60 cells and HL60ρ° cells, activated murine splenic T cells and primary human cells in culture. Phenoxodiol inhibited PMET and cell proliferation of both HL60 cells and activated primary splenic T cells to a similar extent, while HL60ρ° cells were less sensitive. These results support a primary mechanism of action of phenoxodiol that includes PMET and indicate that inhibition of PMET compromises proliferation of both HL60 cells and activated primary immune cells.

2. Materials and methods

2.1. Cells and cell culture

HL60 cells, originally from ATCC, were obtained from Dr. Graeme Findlay (University of Auckland, NZ); WI-38 at passage 7 were from Dr. David Brown (Novogen, Australia), and were expanded from passages 9–10 stocks; primary HUVEC cells at passages 3–4 were from Dr. Sara Gunningham (Christchurch School of Medicine and Health Science, University of Otago). All cell lines used were free of mycoplasma. The mitochondrial DNA-knockout cell line, HL60ρ°, was derived from its parental cell line, HL60, by culturing in the presence of ethidium bromide for 6–8 weeks [17] and lack of mitochondrial DNA verified by PCR and stable phenotype.

Cycling T cells were generated as follows: a single cell suspension of spleens from 8 to 10 weeks old C57BL/6J mice were generated by teasing through a 70 μM cell strainer using IMDM medium containing 5% (v/v) fetal bovine serum, 25 μg/mL penicillin, 25 μg/mL streptomycin and 0.5 μM 2β-mercaptoethanol. Splenocytes, 2×10^6 cells/mL, were stimulated with 0.1 μg/mL 145-2C11 anti-CD3 antibody and 20 μL/mL of 37.51.1 anti-CD28 hybridoma supernatant for 3 days. At this stage, FACS analysis showed that the T cell cultures contained approximately 70% CD8 T cells, 15% CD4 T cells, and 15% other cells (mainly B cells).

For cell surface oxidase assays, T cells were washed twice in HBSS before being used. For MTT assays, T cells were washed twice with complete IMDM medium and incubated with various concentrations of phenoxodiol in the presence of 100 U/mL of IL-2.

All cell lines were grown in RPMI-1640 medium (GIBCO-BRL, Grand Island, NY) supplemented with 5% (v/v) fetal bovine serum, 2 mM glutamate, 25 μg/mL penicillin, 25 μg/mL streptomycin, 50 μg/mL uridine and 1 mM pyruvate to densities of $(1–2) \times 10^6$ cells/mL (exponential stage), at 37 °C in a humidified incubator maintained at 5% CO_2.

2.2. Materials

2-(4-iodophenyl)-3-(4-nitrophenyl)-5-(2,4-disulfophenyl)-2H-tetrazolium monosodium salt (WST-1) and 1-methoxyphenazine methylsulfate (1 mPMS) were purchased from Dojindo Laboratories (Kumamoto, Japan). Phenoxodiol was obtained from Novogen Inc. (NSW, Australia) and Doxorubicin hydrochloride was purchased from Faulding Pharmaceuticals (Warwickshire, UK). Mouse anti-human PE-labelled CD95 (Fas), propidium iodide (PI), fluorescein isothiocyanate (FITC)-labelled Annexin V (AV) and Annexin V binding buffer were from Pharmingen (Becton Dickinson, North Ryde, Australia). The antibody 145-2C11 (anti-CD3εγ/εδ) was purified from culture supernatant. Supernatant from cells transfected with recombinant mIL-2 was used as a source of IL-2. Supernatant from the 37.51.1 hybridoma cell

line was used as a source of anti-CD28. IL-2, anti-CD3, and anti-CD28 was kindly provided by Dr. Thomas Backstrom (Malaghan Institute of Medical Research, Wellington, New Zealand). Unless otherwise stated all other reagents were from Sigma (St. Louis, Missouri, USA). Phenoxodiol was stored in solid form under nitrogen gas to prevent oxidation and dissolved prior to each experiment in DMSO at 10× or 100× the final concentration before being diluted in HBSS or RPMI-1640.

2.3. Mice

C57BL/6J mice were originally purchased from the Jackson Laboratory (Bar Harbour, ME). All mice were maintained by the Biomedical Research Unit at the Malaghan Institute of Medical Research. Experimental protocols were approved by Victoria University Animal Ethics Committee, and performed according to their guidelines.

2.4. PMET activity measured by WST-1/PMS reduction

WST-1/PMS reduction rates were measured in a microplate format as described previously [11]. Briefly, exponentially growing cells were centrifuged at 130 × *g* for 5 min, washed and resuspended in HBSS buffer. For each assay, 50 μL of a 2×10^6 cells/mL cell suspension was pipetted into microplate wells containing 50 μL of the inhibitor/buffer solution (10 μL of a 10× stock solution added to 40 μL of HBSS buffer), resulting in a final concentration of 1×10^6 cells/mL. Dye reduction was initiated by adding 10 μL of a 10× stock solution of WST-1/PMS in MilliQ water (final concentrations of 500 μM WST-1 and 20 μM PMS). WST-1 reduction was measured in real time at 450 nm over 30–60 min in a BMG FLUOstar OPTIMA plate reader.

2.5. Cell surface NADH-oxidase activity measured by WST-1/NADH reduction

Cell surface NADH-oxidase activity [18] was measured as for PMET activity except that 200 μM NADH was used instead of 20 μM PMS in microplate assays. All values were corrected for background readings of cells in the presence of WST-1 and inhibitors (without NADH) as well as for auto-oxidation.

2.6. Cell proliferation measured by MTT reduction

MTT reduction was measured as previously described [19] in a microplate format as follows: exponentially growing cells were centrifuged at 130 × *g* for 5 min, washed and resuspended in HBSS buffer. For each assay, 50 μL of a 1×10^6 cells/mL cell suspension was pipetted into microplate wells containing 50 μL of the inhibitor/buffer solution (10 μL of the 10× stock solution added to 40 μL of HBSS buffer), resulting in a final concentration of 5×10^5 cells/mL. Following 44 h incubation, dye reduction was initiated by adding 10 μL of 5 mg/mL MTT to each well. After 2 h, 100 μL of lysing buffer was added and formazan crystals dissolved by manual pipetting using a multichannel pipette before measuring A570 in a BMG FLUOstar OPTIMA plate reader.

2.7. Trypan blue exclusion

HL60 and HL60ρ° cells were grown to mid-exponential phase in RPMI-1640, centrifuged at 130 × *g* at room temperature for 5 min and resuspended in 10 mL of fresh medium in the absence and presence of phenoxodiol and/or doxorubicin to a density of 2×10^5 cells/mL. Viable cells, as determined by Trypan blue exclusion, were counted in a Neubauer haemocytometer every 24 h for several days.

2.8. Annexin V/ propidium iodide staining

AV/PI double staining was used to distinguish between viable cells (AV^-/PI^-), early apoptotic cells (AV^+/PI^-), early necrotic cells (AV^-/PI^+) and late apoptotoc/dead cells (A^+/PI^+). Cells were centrifuged at 130 × *g* at room temperature for 5 min, washed in phosphate buffered saline solution, pH 7.3 (PBS) and resuspended in Annexin V binding buffer. Small aliquots ((0.5–1) × 10^6 cells) were transferred to 1.5 mL tubes and spun at 2000 rpm for 2 min in a Biofuge Fresco (Kendro, Auckland). Most supernatant was removed and 5 μL PI and 5 μL FITC-labelled AV was added to the wet pellets which were vortexed. After 30 min in the dark on ice, 500 μL of Annexin V binding buffer was added, the cells were centrifuged for 2 min at 2000 rpm, washed once with Annexin V binding buffer and resuspended in 1 mL of binding buffer in FACS tubes. Staining was analyzed by flow cytometry using a Becton Dickinson FACSort with FlowJo software.

2.9. Expression of cell surface markers

Cells were harvested and washed twice with ice-cold FACS buffer (PBS containing 0.01%, w/v, sodium azide). Aliquots of 10^6 cells were incubated in the dark for 30 min on ice with 5 μL of one the fluorescently labelled α-CD95(Fas) or with the appropriate isotype control. Stained cells were washed twice in ice-cold PBS and resuspended in PBS (containing 1%, w/v, paraformaldehyde). Flow cytometry and data analysis were performed as for AV/PI double staining.

2.10. ^{3}H-thymidine incorporation

HL60 and HL60ρ° were washed twice in RPMI-1640, and 2.5×10^4 cells in 200 μL complete IMDM were plated in flat 96-well plates with phenoxodiol at various concentrations in triplicate wells. The cells were incubated at 37 °C and 5% CO_2 for 9, 23, 32, or 56 h with 1 μCi/mL of ^{3}H-thymidine added for the last 9 h of culture.

2.11. Caspase activation

Pan-caspase activation was measured using the fluorescein CaspaTag™ kit from Chemicon (Life Sciences NZ Ltd., Auckland, New Zealand) according to manufacturers' recommendations. Briefly, 0.25×10^6 cells/mL in 5 mL of RPMI-1640 were incubated with phenoxodiol. At the end of incubation, the cells were spun down for 2 min at 2000 rpm and the supernatant was discarded. The cell pellet was resuspended in 200 μL RPMI medium containing phenoxodiol and 0.1× FLICA reagent (FAM-VAD-FMK) and incubated for another 1 h at 37 °C. The

cells were then washed twice with wash buffer, resuspended in 300 μL wash buffer containing propidium iodide to gate out dead cells, and analyzed on a FACS Calibur (Becton Dickinson).

3. Results

3.1. *Effects of phenoxodiol on PMET by HL60, HL60ρ° and primary cells*

The effects of phenoxodiol on PMET by human leukemic HL60 cells and HL60ρ° cells were determined by measuring reduction of the cell-impermeable tetrazolium dye, WST-1 in real time, in the presence of its mandatory intermediate electron acceptor, 1 mPMS. Phenoxodiol inhibited PMET by HL60 cells with an IC_{50} of 32 μM and HL60ρ° cells with an IC_{50} of 70 μM (Fig. 1A; Table 1). To determine whether the effects of phenoxodiol on PMET by HL60 cells were cancer-specific, WST-1 reduction was determined in non-transformed WI-38 human lung fibroblasts, primary HUVECs and activated murine splenic T cells. Unexpectedly, phenoxodiol inhibited PMET by activated splenic T cells with an IC_{50} of 29 μM, similar to that of HL60 cells. In addition, PMET activity by HUVECs and WI-38 cells was also inhibited with IC_{50} values of 74 and 118 μM, respectively. These results indicate that the effects of phenoxodiol on PMET are not tumour-specific.

3.2. *Effects of phenoxodiol on cell surface NADH-oxidase activity in HL60, HL60ρ° and primary cells*

PMET involves an NADH-oxidoreductase at the cytosolic surface of the plasma membrane, membrane ubiquinone and a cell surface NADH-oxidase, so-called because of its ability to oxidize NADH added extracellularly [18]. Fig. 1B shows that phenoxodiol (100 μM) stimulated NADH-dependent reduction of WST-1 by HL60ρ° cells and activated T cells by 80% and that of HL60 cells by 40% but had little effect on the surface NADH-oxidase activity of WI-38 cells and HUVECs. Stimulation of NADH-dependent WST-1 reduction by extracellular reductants is consistent with reduction of ubiquinone to ubiquinol preventing reverse electron flow through the PMET system [20].

3.3. *Effects of phenoxodiol on proliferation and viability and of HL60, HL60ρ° and primary cells*

The physiological significance of phenoxodiol inhibiting PMET activity and stimulating cell surface NADH-oxidase activity was explored by measuring the effects of phenoxodiol on cell proliferation (MTT reduction at 44 h) and cell viability by Trypan blue dye exclusion at times up to 96 h. The proliferation of HL60 cells and activated T cells was more strongly inhibited by phenoxodiol (IC_{50} of 2.8 and 2.5 μM, respectively) than were HL60ρ° cells (IC_{50} of 6.7 μM) (Fig. 2A), while an IC_{50} was not reached with WI-38 or HUVECs (>100 μM). The effects of phenoxodiol (10 μM) on viable cell numbers were also determined over a period of 3 days and showed a differential loss of viable cell numbers that correlated with cycling times. Activated T cells, with a cycling time of 9 h, responded faster than HL60 cells (cycling time 15 h), which in turn responded faster than HL60ρ° cells (cycling time 29 h) (Fig. 2B). In contrast, no significant loss of viable cells was observed with HUVECs (cycling time 30 h) in response to phenoxodiol treatment. ^{3}H-thymidine incorporation by HL60 and HL60ρ° cells at times up to 56 h showed concentration-dependent inhibition by phenoxodiol at all time points (Fig. 2C and D). IC_{50} values for HL60 cells were in the range of 2–2.3 μM and for HL60ρ° cells 5–6.8 μM.

3.4. *Phenoxodiol induces death by apoptosis in HL60 and HL60ρ° cells and in activated splenic T cells*

To determine whether loss of viable cells following exposure of HL60 and HL60ρ° cells to 10 μM phenoxodiol was a consequence of apoptotic cell death, cells were stained with AV and PI at times of up to 5 days (Fig. 3). The percentage of both AV^+ single-stained cells and AV^+/PI^+ double-stained cells increased more rapidly in HL60 than in HL60ρ° cells with the predominant pathway of cell death being apoptosis rather than necrosis. Caspases were activated within 6 h of exposure of HL60 cells to phenoxodiol (38% positive cells), but with

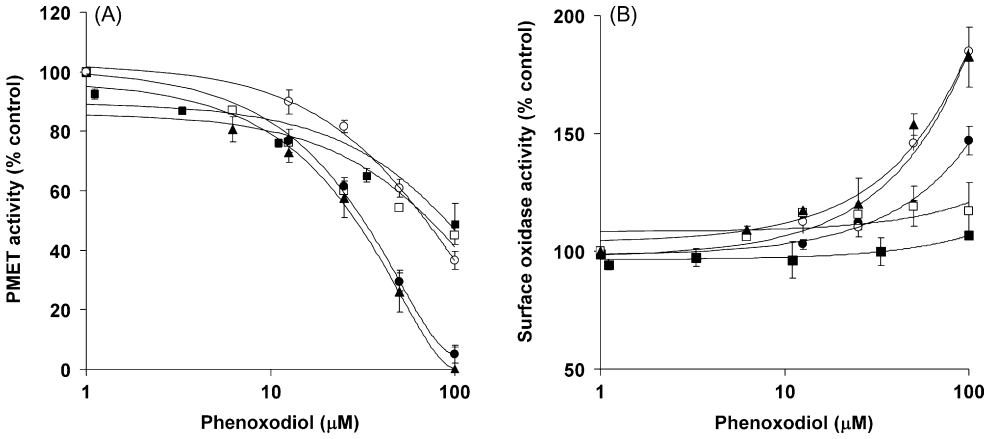

Fig. 1 – Concentration-dependent effects of phenoxodiol on PMET activity (A) and surface oxidase activity (B). Cell lines: HL60 (●), HL60ρ° (○), WI-38 (■), HUVEC (□) and activated T cells (▲). Results are averages ± S.E.M. of at least four independent experiments.

Table 1 – Effect of cycling time on phenoxodiol sensitivity in cells using PMET

	Cycle time (h)	IC_{50} μM MTT	IC_{50} μM PMET	PMET activity*
Activated T cells	9	2.5	29	9.43 ± 0.56
HL60	15	2.8	32	14.80 ± 0.51
HL60ρ°	28	6.7	70	29.93 ± 1.55
WI38	30	>100	74	13.76 ± 0.86
HUVEC	40	>100	118	9.35 ± 0.53

* PMET values are in milliA 450 min^{-1} 10^5 $cells^{-1}$.

HL60ρ° cells a delay of about 33 h was observed before similar caspase levels were attained (Fig. 4). AV/PI double staining of activated murine splenic T cells showed a substantially faster loss of viable cells compared with either HL60 or HL60ρ° cells (Fig. 5), which was in accordance with the results shown in Fig. 2B as well as with their faster cycling time.

3.5. *Effects of phenoxodiol on doxorubicin-induced cytotoxicity of HL60 and HL60ρ° cells*

The ability of phenoxodiol to inhibit both PMET and cell proliferation and to induce apoptotic cell death in HL60 cells suggests that PMET may be a primary target for the anticancer effects of phenoxodiol. To investigate the effects of phenoxodiol on the anticancer effects of another well-established redox-active anticancer drug, doxorubicin, HL60 and HL60ρ° cells were treated with a non-toxic concentration of 1 μM phenoxodiol in the presence and absence of 0.016 μM doxorubicin and viable cell numbers followed. With both HL60 and HL60ρ° cells the cytotoxic effects of doxorubicin were enhanced by phenoxodiol in a synergistic manner (Fig. 6). It is noteworthy that HL60ρ° cells exhibited considerable resistance to doxorubicin, an observation that suggests that most of the cytotoxic effect of

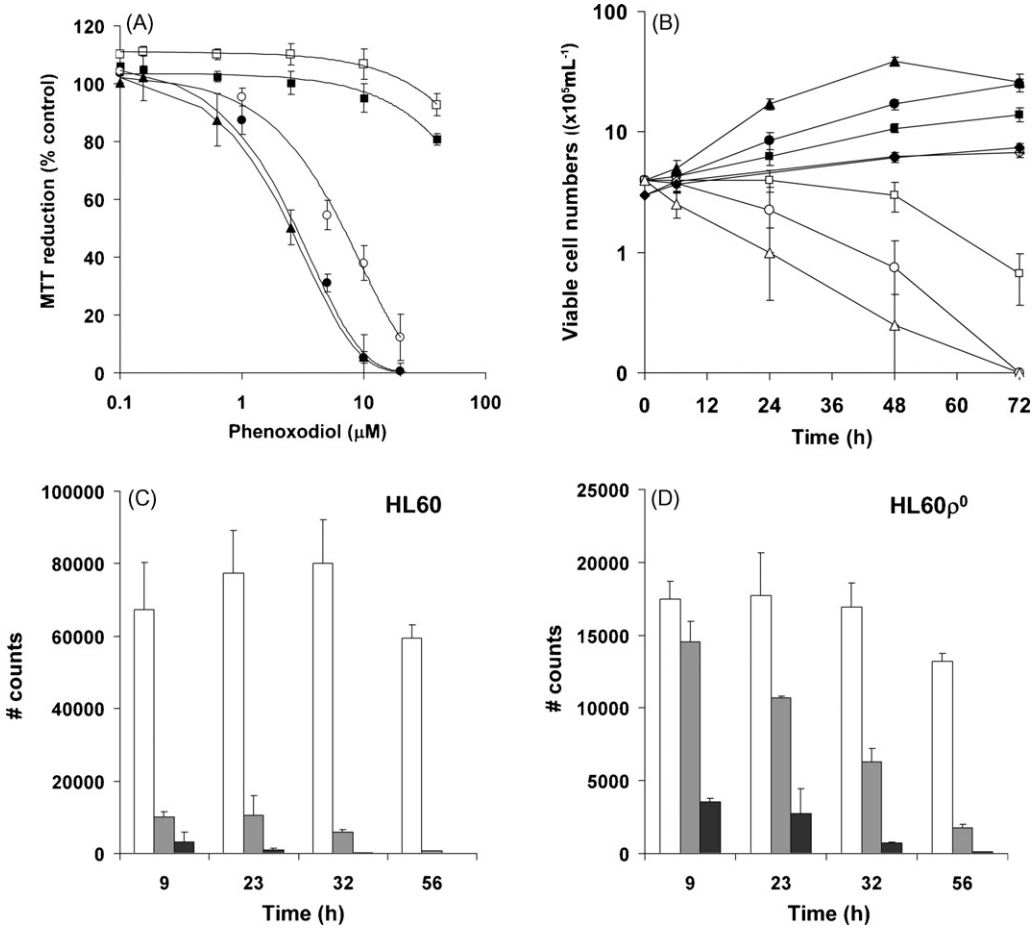

Fig. 2 – Effects of phenoxodiol on cell proliferation (A and B) and DNA synthesis (C and D). (A) MTT reduction after 44 h, cell lines: HL60 (●), HL60ρ° (○), WI-38 (■), HUVEC (□) and activated T cells (▲). (B) Number of viable cells as measured by Trypan blue exclusion, cell lines: HL60 (●), HL60 + 10 μM PXD (○), HL60ρ° (■), HL60ρ° + 10 μM PXD (□), T cells (▲), T cells + 10 μM PXD (△), HUVEC (◆), HUVEC + 10 μM PXD (◇). (C and D) ^{3}H-thymidine incorporation before (white bars) and after exposure to 3.3 μM (grey bars) and 10 μM PXD (black bars) in HL60 cells (C) and HL60ρ° cells (D). Results are averages ± S.E.M. of four (A and B) experiments and the average and S.D. of one experiment (C and D).

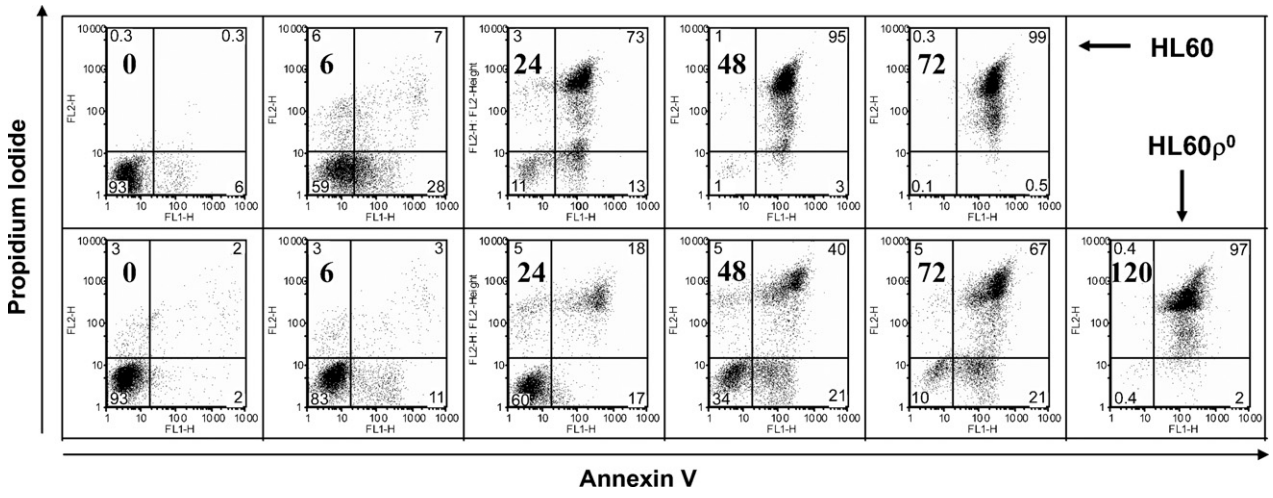

Fig. 3 – Effects of phenoxodiol (PXD) on cell viability of HL60 and HL60ρ°. AV/PI double staining was performed on HL60 (top panel) and HL60ρ° cells (bottom panel) before and exposure to 10 μM PXD for different periods of time; bold figures on the plots represent hours of exposure. AV^-/PI^-: percentage viable cells, AV^+/PI^-: percentage early apoptotic cells, AV^-/PI^+: percentage early apoptotic cells, AV^+/PI^+: percentage late apoptotic and dead cells. Results are representative of four separate experiments.

doxorubicin on HL60 cells may be mediated by MET rather than by PMET.

4. Discussion

The question of whether PMET is a target for the anticancer drug, phenoxodiol, was addressed, in this study, by directly measuring reduction of the extracellular tetrazolium dye, WST-1. Strong inhibition of dye reduction by phenoxodiol was observed with activated splenic T cells, HL60 cells, and to a lesser extent with HL60ρ° cells. Although HL60ρ° cells have elevated PMET compared with HL60 cells [11], they have a longer cell cycle time that could in part explain their reduced sensitivity to phenoxodiol. In addition, it is likely that the mechanism of action of phenoxodiol includes sites other than PMET. Inhibition of PMET by phenoxodiol was associated with inhibition of cell proliferation that was also most profound in activated T cells and HL60 cells. IC_{50} values for HL60, HL60ρ°, and T cell proliferation were about an order of magnitude lower than IC_{50} for PMET (Table 1), consistent with cumulative effects over the longer time-course of the cell proliferation assay (2 days) compared with PMET assays (1 h). In contrast to HL60, HL60ρ° and T cells, PMET activity, surface NADH-oxidase activity and proliferation of WI-38 cells and HUVECs were relatively unaffected by phenoxodiol. Thus, sensitivity to phenoxodiol is closely associated with cell growth rate (Table 1) particularly in cell types that rely on PMET to recycle NADH in order to combat intracellular reductive stress [9]. More recently, we have observed that human peripheral blood mononuclear cells, activated to proliferate rapidly in culture with anti-CD3, anti-CD28 and IL-2, are also sensitive to phenoxodiol, with IC_{50} values for PMET and MTT proliferative responses commensurate with their longer cell cycle time (Herst and Berridge, manuscript in preparation).

Previously, phenoxodiol has been shown to bind to and inhibit the activity of a recombinant tumour-specific NADH-oxidase from HeLa cells [13] that is thought to be involved in PMET. However, in that study, PMET activity was not measured directly. Rather, inhibition of growth of HeLa cervical carcinoma cells (IC_{50} of 0.2 μM) and BT-20 mammary carcinoma cells (IC_{50} of 2 μM) was demonstrated. In contrast, growth of non-cancer MCF-10A mammary cells was unaffected by phenoxodiol ($IC_{50} > 20$ μM). The non-sigmoidal nature of the growth response curves presented are, however, suggestive of a complex mechanism of action.

In our studies, inhibition of PMET by phenoxodiol was associated with increased cell surface NADH-oxidase activity. This dichotomy in the response of a cell surface-associated component of PMET and PMET itself, to a PMET inhibitor, has been observed previously [18,20] and has been attributed to perturbation of the redox status of membrane ubiquinone in favor of ubiquinol, thus increasing the ability of extracellular NADH to reduce WST-1 outside the cell via a competing pathway [20].

Our results do not support the view that phenoxodiol is tumour-specific [7,13], but do indicate a hierarchy of sensitivities of primary cells to the drug, with activated primary T cells being highly sensitive to phenoxodiol and WI-38 cells and HUVECs being relatively insensitive. These results suggest that at concentrations of phenoxodiol that are effective in compromising the proliferation of tumour cells, immunosuppressive effects can be anticipated in preclinical and clinical studies. Indeed, immunosuppressive effects were recently reported in a Phase I clinical trial with 19 out of 21 patients experiencing lymphocytopenia at doses up to 30 mg/kg [2].

Loss of viable cells in response to phenoxodiol exposure was associated with increased markers of apoptosis including Annexin V expression and pan-caspase activity, and these effects were less pronounced with slower growing, purely

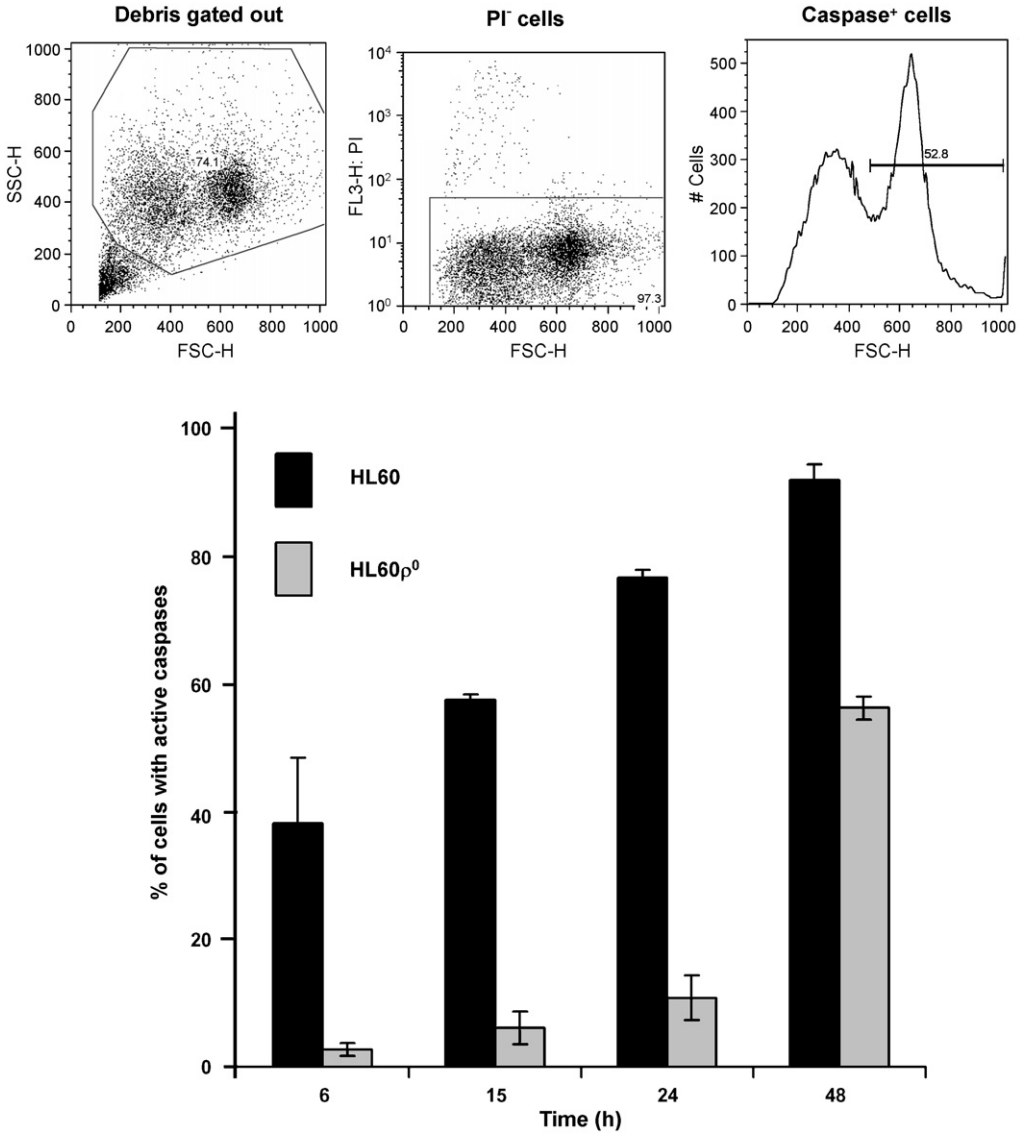

Fig. 4 – Effects of phenoxodiol on caspase activation in HL60 and HL60ρ° cells. Cells were exposed to 10 μM phenoxodiol for periods of up to 2 days and caspase 3 activity was measured in the presence of FLICA reagent of the CaspaTag™ kit. Results are averages ± S.E.M. from two separate experiments except for the 24 h time point where *n* = 3. At this time point, the paired two-tailed Student *t*-test for the difference between the percentage of caspase-activated HL60 and HL60ρ° cells gave a *p* value of <0.0001.

glycolytic HL60ρ° cells than with parental HL60 cells. Substituting phenoxodiol with equol, an inactive analogue of phenoxodiol saturated across the unconjugated double bond in the phenoxy ring gave results that were similar to the buffer control in PMET and cell proliferation assays (results not shown). The link between inhibition of PMET by phenoxodiol and induction of apoptosis is not known.

Thus, phenoxodiol has been shown to induce proteosomal degradation of the caspase inhibitory proteins, XIAP, in primary ovarian cancer [3,4] and melanoma cells [5] by a mechanism involving Akt signalling [4], and to disrupt FLICE inhibitory protein expression in ovarian cancer cells [4]. However, the molecular target(s) of phenoxodiol that result in apoptosis remain unclear. De Luca et al. [7] proposed that inhibition of tumour-specific tNOX by phenoxodiol and several other anticancer compounds compromises PMET resulting in increased cellular NADH and membrane ubiquinol which inhibits sphingosine kinase, inducing G1 arrest and apoptosis. If this mechanism pertains, then phenoxodiol cannot act specifically on tNOX or cancer cells since the proliferation of activated T cells is also inhibited, and cell death also occurs through apoptosis in these primary cells. In support of this view, Gamble et al. [21] recently demonstrated that phenoxodiol exhibits potent anti-angiogenic properties, inhibiting endothelial cell proliferation, migration and capillary tube formation, questioning cancer cell specificity and indicating that the anticancer properties of phenoxodiol are complex with multiple targets.

In summary, our results are consistent with PMET being a primary site of action of phenoxodiol in tumour cells and in primary T cells. We propose that sensitivity to phenoxodiol

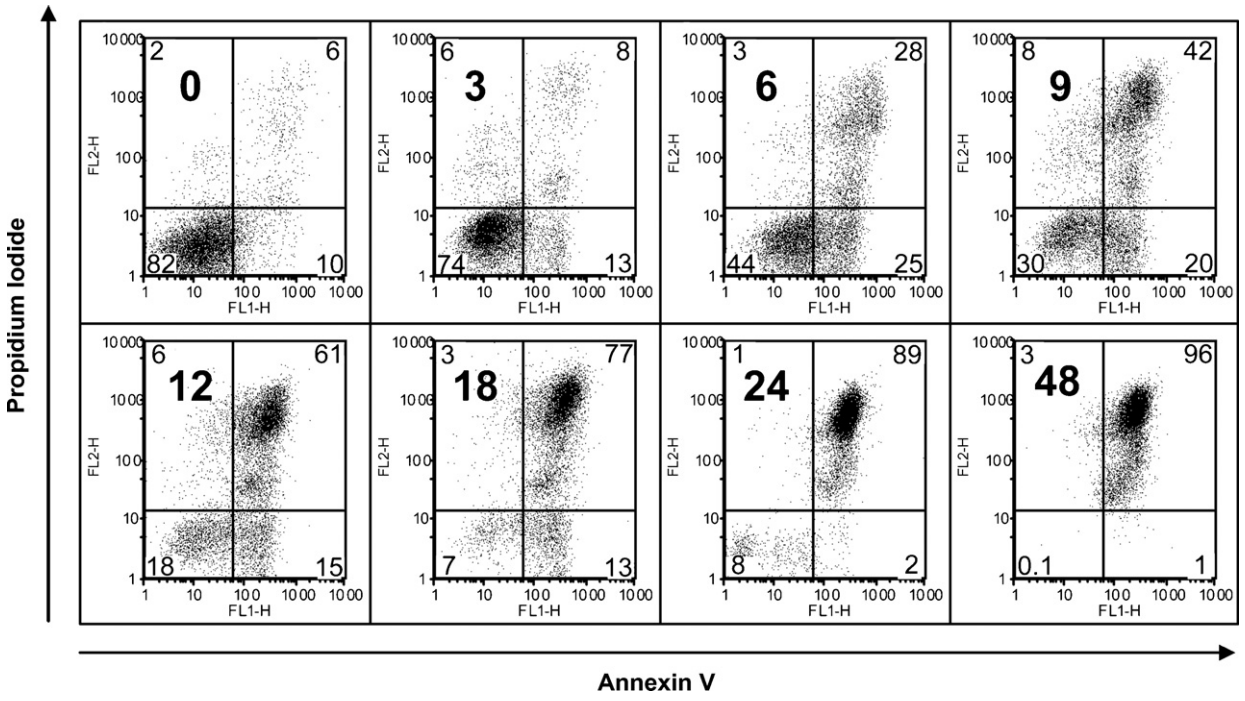

Fig. 5 – Effects of phenoxodiol on cell viability of activated murine splenic T cells. AV/PI double staining was performed on activated murine splenic T cells before and after exposure to 10 μM PXD for different periods of time; bold figures on the plots represent hours of exposure. AV^-/PI^-: percentage viable cells, AV^+/PI^-: percentage early apoptotic cells, AV^-/PI^+: percentage early apoptotic cells, AV^+/PI^+: percentage late apoptotic and dead cells. Results are representative of three separate experiments.

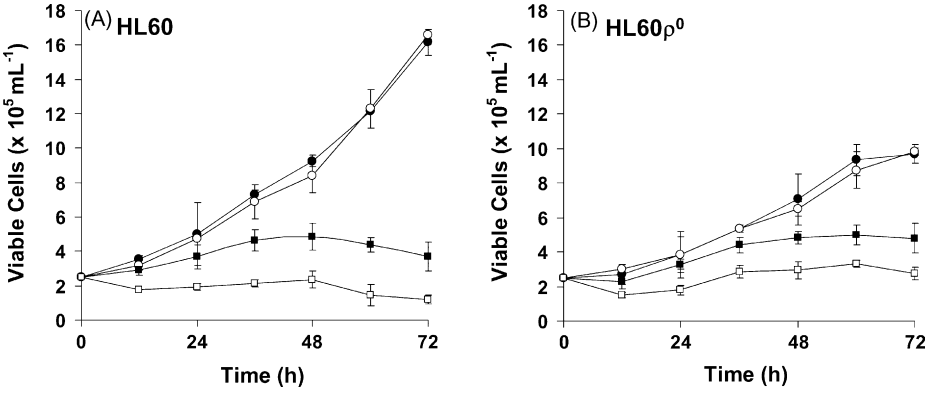

Fig. 6 – The effect of sub-lethal doses of phenoxodiol alone or in combination with doxorubicin on proliferation of HL60 (A) and HL60ρ° cells (B). Cells were grown in the absence (●) and presence of 1 μM PXD (○), 0.016 μM DOX (■) and 1 μM PXD + 0.016 μM DOX (□) over 4 days. Cell viability was assessed by Trypan blue exclusion. Results are averages ± S.E.M. of three separate experiments.

depends on the extent to which cells are dependent on PMET for maintaining a favorable intracellular NADH/NAD^+ ratio to support cellular bioenergetics, regardless of the transformation status of the cell.

Acknowledgements

This research was supported by Marshall Edwards Inc., the Cancer Society of New Zealand, by Genesis Oncology Trust and by the Department of Radiation Therapy, Wellington School of Medicine and Health Sciences, University of Otago.

REFERENCES

[1] Constantinou AI, Husband A. Phenoxodiol (2H-1-benzopyran-7-0,1,3-(4-hydroxyphenyl)), a novel isoflavone derivative, inhibits DNA topoisomerase II by stabilizing the cleavable complex. Anticancer Res 2002;22(5):2581–5.

[2] Choueiri TK, Mekhail T, Hutson TE, Ganapathi R, Kelly GE, Bukowski RM. Phase I trial of phenoxodiol delivered by continuous intravenous infusion in patients with solid cancer. Ann Oncol 2006;17(5):860–5.
[3] Alvero AB, O'Malley D, Brown D, Kelly G, Garg M, Chen W, et al. Molecular mechanism of phenoxodiol-induced apoptosis in ovarian carcinoma cells. Cancer 2006;106(3):599–608.
[4] Kamsteeg M, Rutherford T, Sapi E, Hanczaruk B, Shahabi S, Flick M, et al. Phenoxodiol – an isoflavone analog – induces apoptosis in chemoresistant ovarian cancer cells. Oncogene 2003;22(17):2611–20.
[5] Kluger HM, McCarthy MM, Alvero AB, Sznol M, Ariyan S, Camp RL, et al. The X-linked inhibitor of apoptosis protein (XIAP) is up-regulated in metastatic melanoma, and XIAP cleavage by phenoxodiol is associated with carboplatin sensitization. J Trans Med 2007;5:1–15.
[6] Aguero MF, Facchinetti MM, Sheleg Z, Senderowicz AM. Phenoxodiol, a novel isoflavone, induces G1 arrest by specific loss in cyclin-dependent kinase 2 activity by p53-independent induction of p21WAF1/CIP1. Cancer Res 2005;65(8):3364–73.
[7] De Luca T, Morré DM, Zhao H, Morré DJ, Davies SL, Bozzo J. NAD+/NADH and/or CoQ/$CoQH_2$ ratios from plasma membrane electron transport may determine ceramide and sphingosine-1-phosphate levels accompanying G1 arrest and apoptosis. Biofactors 2005;25(1–4):43–60.
[8] Pelicano H, Xu RH, Du M, Feng L, Sasaki R, Carew JS, et al. Mitochondrial respiration defects in cancer cells cause activation of Akt survival pathway through a redox-mediated mechanism. J Cell Biol 2006;175(6):913–23.
[9] Herst PM, Berridge MV. Plasma membrane electron transport: a new target for cancer drug development. Curr Mol Med 2006;6:895–904.
[10] Ly JD, Lawen A. Transplasma membrane electron transport: enzymes involved and biological function. Redox Rep 2003;8(1):3–21.
[11] Berridge MV, Tan AS. High-capacity redox control at the plasma membrane of mammalian cells: trans-membrane, cell surface, and serum NADH-oxidases. Antiox Redox Signal 2000;2:231–42.
[12] Herst PM, Tan AS, Scarlett DJ, Berridge MV. Cell surface oxygen consumption by mitochondrial gene knockout cells. Biochim Biophys Acta 2004;1656(2–3):79–87.
[13] Morré DJ, Chueh P-J, Yazig K, Balicki A, Kim C, Morré DM. ECTO-NOX target for the anticancer isoflavene phenoxodiol. Oncology Research 2007;16: 299–312.
[14] Chueh PJ, Kim C, Cho N, Morré DM, Morré DJ. Molecular cloning and characterization of a tumor-associated, growth-related, and time-keeping hydroquinone (NADH) oxidase (tNOX) of the HeLa cell surface. Biochemistry 2002;41(11):3732–41.
[15] Morré DJ, Sedlak D, Tang X, Chueh PJ, Geng T, Morré DM. Surface NADH oxidase of HeLa cells lacks intrinsic membrane binding motifs. Arch Biochem Biophys 2001;392(2):251–6.
[16] Scarlett D-JG, Herst PM, Tan AS, Prata C, Berridge MV. Mitochondrial gene-knockout (ro) cells: a versatile model for exploring the secrets of trans-plasma membrane electron transport. Biofactors 2004;20:213–20.
[17] King MP, Attardi G. Human cells lacking mtDNA: repopulation with exogenous mitochondria by complementation. Science 1989;246(4929):500–3.
[18] Berridge MV, Tan AS. Cell-surface NAD(P)H-oxidase: relationship to trans-plasma membrane NADH-oxidoreductase and a potential source of circulating NADH-oxidase. Antiox Redox Signal 2000;2:277–88.
[19] Berridge MV, Tan AS. Trans-plasma membrane electron transport: a cellular assay for NADH- and NADPH-oxidase based on extracellular, superoxide-mediated reduction of the sulfonated tetrazolium salt WST-1. Protoplasma 1998;205(1–4):74–82.
[20] Scarlett DJ, Herst PM, Berridge MV. Multiple proteins with single activities or a single protein with multiple activities: the conundrum of cell surface NADH oxidoreductases. Biochim Biophys Acta 2005;1708(1):108–19.
[21] Gamble JR, Xia P, Hahn CN, Drew JJ, Drogemuller CJ, Brown D, et al. An experimental anticancer drug, shows potent antiangiogenic properties in addition to its antitumour effects. Int J Cancer 2006;118(10): 2412–20.